INVERTING INPUT SCANNER VIBRATION ERRORS

George Wolberg
Department of Computer Science
City College of New York / CUNY
New York, NY 10031
wolberg@cs-mail.engr.ccny.cuny.edu

Robert P. Loce
Xerox Corporation
Corporate Research and Technology
Webster, NY 14580
loce.wbst147@xerox.com

ABSTRACT

Images scanned in the presence of mechanical vibrations are subject to artifacts such as brightness fluctuation and geometric warping. The goal of this work is to develop an algorithm to invert these distortions and produce an output digital image consistent with a scanner operating under ideal uniform motion conditions. The image restoration algorithm described in this paper applies to typical office scanners that employ a moving linear sensor array (LSA) or moving optics. The velocity of the components is generally not constant in time. Dynamic errors are introduced by gears, timing belts, motors, and structural vibrations.

In this work, we make use of the instantaneous LSA velocity to reconstruct an underlying piecewise constant or piecewise linear model of the image irradiance function. The control points for the underlying model are obtained by solving a system of equations derived to relate the observed area samples with the instantaneous LSA velocity and a spatially-varying sampling kernel. An efficient solution exists for the narrow band diagonal matrix that results. The control points computed with this method fully define the underlying irradiance function. That function is then suitable for resampling under ideal scanning conditions to produce a restored image.

1. INTRODUCTION

In a document scanner, a linear sensor array (LSA) passes over a document, ideally, at uniform velocity. The output of a single photosensor in the LSA is proportional to the integrated irradiance received by the sensor as it scans through an exposure region. When vibratory motion of the sensor array is considered, the actual size of the exposure region is time-varying. This introduces artifacts such as brightness fluctuation and geometric warping. In this paper, we develop a digital image restoration algorithm to invert these distortions and produce output consistent with a scanner that is not subjected to vibrations. For more details, the reader is referred to [1,2]. A related paper [3] examines the artifacts induced by vibrations for several image types.

2. THE PROBLEM OF INPUT SCANNER VIBRATIONS

Consider the output of a single photosensor in an LSA. Let $H(x)$ be the image irradiance distribution, and let $S(x - X(t))$ be the static photosensor sensitivity profile (i.e., rect PSF) positioned at $X(t)$ at time t. The instantaneous charge $C(X(t))$ generated by the photosensor is given by a convolution: $C(X(t)) = H(X(t)) * S(-X(t))$. Digitization is performed by integrating, or accumulating, C for a period of time T_{acc}, and then sampling it at temporal intervals T_s, where $T_{acc} \le T_s$. The nth sample is given by

$$F(n) = \int_{nT_s}^{nT_s+T_{acc}} H(X(t))*S(-X(t))\,dt = \sum_n \delta(t - nT_s)\left[H(X(t)) * K(t)\right]$$

where $K(t) = rect(t / T_{acc}) * S(-X(t))$ and $rect(t) = 1$ for $-0.5 < t \le 0.5$ and 0 otherwise.

The accumulated charge is seen to be the convolution of the image irradiance distribution H with a kernel K that combines the effects of sensitivity function S and the motion blur incurred during the accumulation time T_{acc}. While S may be referred to as the *static integration aperture*, we refer to K as the *dynamic integration aperture* because it takes motion blur into account. If we assume that S is rectangular in form and the LSA is moving at uniform velocity during the accumulation time, then K takes a trapezoidal form.

The sampling electronics digitize H over equal intervals in time. It is therefore straightforward to write the collection of samples as a temporal function, as seen above. However, we are interested in the effect of vibratory motion on the digitized image. For the purpose of analyzing image defects, the influence of vibration is best understood by recasting F in terms of spatial coordinate x. Since LSA velocity nonuniformity tends to be periodic, it is convenient to express velocity $V(t)$ as a Fourier series:

$$V(t) = V_0 + \sum_i A_i \sin(2\pi f_i t + \phi_i),$$

where A_i, f_i, and ϕ_i are the velocity error amplitude, temporal frequency, and phase, respectively, for the ith frequency component. The velocity error amplitudes are typically less than 1% of the nominal velocity V_0.

We can express $F_{vib}(X)$, the samples taken in the presence of vibrations, as

$$F_{vib}(X) = \sum_n W_n \left[H(X) * K_{vib}(X)\right] \delta(X - nX_s),$$

where

$$K_{vib}(X) = S(X) * rect\left[\frac{X}{2\xi_{n,ctr}}\right],$$

$$W_n = V_0^{-1} - V_0^{-2} \sum_i A_i \sin(2\pi\beta_i(nX_s + \xi_{n,ctr}) + \phi_i).$$

The terms $\xi_{n,0}$ and $\xi_{n,1}$ denote the spatial deviations of the LSA from the nominal positions at time nT_s and $nT_s + T_{acc}$, respectively. These position errors are defined as

$$\xi_{n,0} = \sum_i \frac{A_i}{2\pi f_i} \left[\cos(\phi_i) - \cos(2\pi f_i n T_s + \phi_i)\right],$$

$$\xi_{n,1} = \sum_i \frac{A_i}{2\pi f_i} \left[\cos(\phi_i) - \cos(2\pi f_i n T_s + T_{acc} + \phi_i)\right].$$

The term $\xi_{n,ctr}$ denotes the center of the span traversed in interval n: $\xi_{n,ctr} = (X_{acc} + \xi_{n,1} - \xi_{n,0}) / 2$ where $X_{acc} = V_0\, T_{acc}$ is the nominal distance spanned in one time interval T_{acc}.

As in the uniform velocity case, an idealized rectangular approximation of S results in a trapezoidal form for K. However, in the present nonuniform velocity case, the dimensions and offset of the trapezoid varies for each sample point. Note that W_n scales the trapezoid such that its height is inversely proportional to its width. A good approximation to W_n is the linear expression $1 / (X_{acc} + \xi_{n,1} - \xi_{n,0})$.

3. IMAGE RESTORATION: RECTANGULAR KERNEL

Consider a stream of area samples produced by a photosensor that moves across a document at uniform velocity. Assume that S is sufficiently narrow so that we may approximate the trapezoid kernel K to be a *rect* function. In that case, each area sample is the unweighted integral of the image irradiance function spanned during the charge accumulation time. Furthermore, assume that the accumulation time and the sampling period is the same, i.e., the time needed to read and clear the charge is negligible ($T_{acc} \approx T_s$). In the ideal case of uniform LSA velocity, samples produced at regular intervals T_s in time relate to the areas under H at regular intervals in space. When the sensor travels at nonuniform velocity, samples produced at regular intervals in time relate to the areas under H at irregular intervals in space. The same input now yields different output values.

The image restoration algorithm that we propose infers the underlying image irradiance distribution from the area samples so that we may resample H (or actually re-integrate) at regular intervals in space. Unfortunately, even with precise knowledge of the instantaneous LSA velocity $V(t)$, this problem is underconstrained. We therefore model the irradiance distribution H to consist of piecewise linear segments with control points at regular intervals. This makes it possible to precisely infer H given the area samples F_n and positions x_n that delimit the nonuniform intervals.

The main task in restoring the image is to recover the regularly-spaced control points y_n of the linear spline. Once the control points are determined, H may be reconstructed as a linear spline and area samples can be easily computed at regular intervals. In this manner, we produce output consistent with that of an ideal scanner.

Before delving into the computation of y_n, we first discuss the relation between area samples and the control points. Area samples and position information are collected at regular time intervals. One important assumption is that two consecutive LSA positions must either lie in the same linear spline segment or straddle two segments. Figure 1 depicts both cases, with points A and B denoting the endpoints of the accumulation interval. The next two sections relate the area samples, F_n, to the unknown linear spline control points, y_n, which we seek to recover for each case. The full derivations may be found in [1].

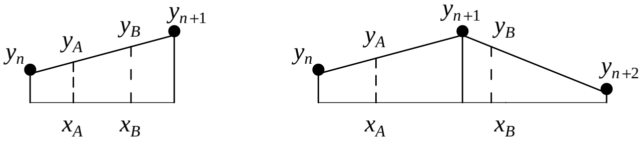

(a) (b)

Figure 1: Two area sampling cases.

3.1 Case 1: *A* and *B* Lie in One Spline Segment

$$\frac{2F_n}{W_n} = y_n \left[k_1(k_2 - 2)\right] + y_{n+1} \left[-k_1 k_2\right]$$

where $k_1 = x_A - x_B$, $k_2 = x_A + x_B$, and W_n, derived earlier, is the normalization term that is inversely proportional to the exposure region.

3.2 Case 2: *A* and *B* Straddle Two Spline Segments

$$\frac{2F_n}{W_n} = y_n \left[(1 - x_A)^2\right] + y_{n+1} \left[1 - x_A^2 + (2 - x_B)x_B\right] + y_{n+2} \left[x_B^2\right].$$

3.3 Solving for the Control Points

Given either of the two cases for the positions of A and B, we have the above expressions to relate each area sample with the neighboring control points. Collectively, they yield a tridiagonal system of equations $\mathbf{K\,Y} = \mathbf{F}$ where K consists of the weights of y_{i-1}, y_i, and y_{i+1}. They are expressed in terms of the known x_A and x_B positions. The control points in $\mathbf{Y}$ are evaluated by multiplying the known area samples $\mathbf{F}$ with the inverse of the tridiagonal matrix $\mathbf{K}$. That is, $\mathbf{Y} = \mathbf{K}^{-1}\mathbf{F}$. The inversion of tridiagonal matrix $\mathbf{K}$ has an efficient algorithm that is solvable in linear time.

4. IMAGE RESTORATION: TRAPEZOIDAL KERNEL

The tridiagonal system of equations derived above is a consequence of two assumptions: consecutive LSA positions never span more than two spline segments, and the LSA sensitivity function S is an impulse (i.e., kernel K is a *rect* function). For the given image model the former assumption is justifiable because the nonuniform LSA velocity generally does not exceed 1% of the nominal velocity. The latter assumption, however, is generally not true since infinitesimally narrow point spread functions (static integration apertures) are difficult to realize. Since the width of S is generally similar to that of X_{acc}, kernel K is trapezoidal, and very nearly triangular.

Figure 2a depicts the three intervals of a trapezoid, delimited by points x_0, x_1, x_2, and x_3. Note that the trapezoid extends beyond LSA positions x_A and x_B, thereby widening the accumulation interval.

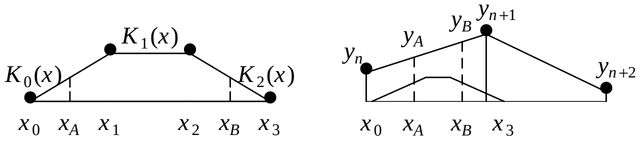

(a) (b)

Figure 2: (a) Kernel *K*; (b) *K* applied to data.

Each observed area sample is now a weighted integral that may be computed in parts:

$$F_n = W_n \int_{x_0}^{x_3} H(x)\,K(x)\,dx = W_n \sum_{i=0}^{2} \int_{x_i}^{x_{i+1}} H(x)\,K_i(x)\,dx\,.$$

Integrating over the three intervals separately permits us to use the previous results in computing the unknown linear spline control points. Rather than considering points *A* and *B*, we consider whether x_i and x_{i+1} lie in one or two spline segments, for $0 \le i \le 2$. The next two sets of equations yield a relationship between F_{n_i} and the unknown control points for both straddling cases.

4.1 Case 1: Trapezoid Interval Lies in One Segment

$$\frac{6F_{n_0}}{W_n} = y_n \left[x_0^2 - 2x_1^2 + x_0 x_1 - 3x_0 + 3x_1\right] + y_{n+1} \left[-x_0^2 + 2x_1^2 - x_0 x_1\right],$$

$$\frac{2F_{n_1}}{W_n} = y_n \left[x_1^2 - x_2^2 - 2x_1 + 2x_2\right] + y_{n+1} \left[-x_1^2 + x_2^2\right],$$

$$\frac{6F_{n_2}}{W_n} = y_n \left[2x_2^2 - x_3^2 - x_2 x_3 - 3x_2 + 3x_3\right] + y_{n+1} \left[-2x_2^2 + x_3^2 + x_2 x_3\right].$$

4.2 Case 2: Trapezoid Interval Straddles Two Segments

$$\frac{6F_{n_0}}{W_n} = y_n \left[k_0^2\right] + y_{n+1} \left[(x_0+2)(1-x_0) + x_1(3-2x_1)\right] + y_{n+2} \left[2x_1^2\right],$$

$$\frac{2F_{n_1}}{W_n} = y_n \left[k_1^2\right] + y_{n+1} \left[1 - x_1^2 + (2-x_2)x_2\right] + y_{n+2} \left[x_2^2\right],$$

$$\frac{6F_{n_2}}{W_n} = y_n \left[2k_2^2\right] + y_{n+1} \left[(2x_2+1)(1-x_2) + x_3(3-x_3)\right] + y_{n+2} \left[x_3^2\right].$$

where $k_i = (1-x_i)$ for $0 \le i \le 2$.

4.3 Solving for the Control Points

Each area sample is actually composed of three contributions: one from each of the three intervals of the trapezoid kernel *K*. Each trapezoid interval, depending on whether it lies in one or two spline segments, adds a constraint to two or three linear spline control points, respectively. Since the three intervals each constrain an overlapping set of three control points, there may be up to five neighboring points that contribute to each area sample. Collectively, they yield a pentadiagonal system of equations. The control points are evaluated by solving the system of equations using LU decomposition optimized for band diagonal matrices.

5. RESULTS

Consider the periodic line image of Fig. 3a, with a spatial period of 1.48 cycles/mm that digitizes to four black and four white pixels at 300 spi. Figure 3c employs the scanner simulation equations with a single frequency of vibration at 1 cycle/mm with a velocity amplitude error of 20%. The lowest beat frequency occurs at 0.48 cycle/mm and is the most noticeable image defect. Note that extremely large errors were used here to render the defects in an obvious form. The restored output, shown in Fig. 3e, is visually indistinguishable from the original input in Fig. 3a.

Figures 3b and 3d show a digitized halftoned image degraded with the same vibration frequency but with a larger velocity amplitude error of 30%. Again, the restored image (Fig. 3f) is visually indistinguishable from the input image in Fig. 3d. For this particular halftone frequency, the vibration defect is not as noticeable as in the periodic line image. A study of the halftone sensitivity to different halftone screen frequencies and orientations is the subject of future work.

6. SUMMARY

Images scanned in the presence of mechanical vibrations are subject to artifacts such as brightness fluctuation and geometric warping. This work has demonstrated how to invert these distortions and produce output consistent with a scanner operating under ideal conditions. The proposed image restoration algorithm makes use of the instantaneous velocity of the LSA to reconstruct an underlying piecewise linear model of the irradiance distribution. That reconstructed image is then suitable for resampling under ideal scanning conditions to produce the restored output.

7. ACKNOWLEDGEMENTS

This work was supported in part by NSF PYI award IRI-9157260, PSC-CUNY grant RF-665313, and a grant from the Xerox Foundation.

8. REFERENCES

[1] G. Wolberg and R. Loce, ‘‘Restoration of Images Degraded by Input Scanner Vibrations,’’ *Journal of Electronic Imaging*, vol. 5, no. 1, Jan. 1996.

[2] G. Wolberg and R. Loce, ‘‘Restoration of Images Degraded by Input Scanner Vibrations,’’ *SPIE Conf. on Document Processing II*, Proc. SPIE 2422, pp. 358-369, Feb. 1995.

[3] R. Loce and G. Wolberg, ‘‘Characterization of Vibration-Induced Image Defects in Input Scanners,’’ *SPIE Conf. on Document Processing II*, Proc. SPIE 2422, pp. 350-357, Feb. 1995.